Bioorganic & Medicinal Chemistry 18 (2010) 1526–1535

Contents lists available at ScienceDirect

Bioorganic & Medicinal Chemistry

journal homepage: www.elsevier.com/locate/bmc

Synthesis, photophysical properties and photocytotoxicity of mono-, di-, tri- and tetra-glucosylated fluorophenylporphyrins

Shiho Hirohara [a,*], Masataka Nishida [a], Kohei Sharyo [a], Makoto Obata [b], Tsuyoshi Ando [a], Masao Tanihara [a]

[a] Graduate School of Materials Science, Nara Institute of Science and Technology, Takayama 8916-5, Ikoma, Nara 630-0192, Japan
[b] Interdisciplinary Graduate School of Medicine and Engineering, University of Yamanashi, Takeda 4-4-37, Kofu 400-8510, Japan

ARTICLE INFO

Article history:
Received 21 November 2009
Revised 31 December 2009
Accepted 5 January 2010
Available online 11 January 2010

Keywords:
Photodynamic therapy (PDT)
S-Glucosylated porphyrin
Photocytotoxicity
Cellular uptake
Reactive oxygen species (ROS)

ABSTRACT

In order to explore the effect of substitution patterns on the photocytotoxicity of glycoconjugated porphyrins, we synthesized and characterized a 'complete set' of tetrakis(perfluorophenyl)porphyrins having β-D-glucopyranosylthio groups on the phenyl ring. Among five possible derivatives, *trans*-substituted S-glucosylated porphyrin *trans*-**2**$_{OH}$ exerted outstanding photocytotoxicity (EC_{50} value was <5 nM) in HeLa cells. The excellent photocytotoxicity of *trans*-**2**$_{OH}$ was found to be attributable to several factors, namely high optical transition probability in aqueous media, efficient type I photoreactions and enhanced cellular uptake.

1. Introduction

Photodynamic therapy (PDT) is a new modality for cancer treatment in which irradiation of cancer cells that have accumulated photosensitizers photochemically generate highly cytotoxic singlet oxygen ($^1O_2$).[1–6] Because the efficacy of PDT treatment crucially depends on the photosensitizer used, the development of an efficient photosensitizer in terms of tumor-selectivity and reactive oxygen species (ROS)-producing ability is very important.

Porphyrin and phthalocyanine derivatives are the most versatile photosensitizers in PDT applications. Because of the highly hydrophobic nature of these photosensitizers, hydrophilic substituents such as sulfonyl groups need to be introduced into the structure of these photosensitizers. It was found that the number and pattern of the hydrophilic substituents affects not only the water-solubility, but also the efficacy of the PDT action. For example, Kessel and MacDonald reported the effects of the substitution pattern of sulfonyl groups on the cellular uptake and photocytotoxicity of tetraphenylporphyrin tetrasulfonic acid (TPPS) derivatives ($TPPS_1$, $TPPS_{cis2}$, $TPPS_{trans2}$, $TPPS_3$ and $TPPS_4$) and aluminum phthalocyanine (AlPcS) derivatives ($AlPcS_1$, $AlPcS_{cis2}$, $AlPcS_{trans2}$, $AlPcS_3$ and $AlPcS_4$).[7–10] They found that the PDT effect of these photosensitizers was significantly dependent on the substitution pattern of the hydrophilic sulfonyl groups, with the *cis*-disubstituted ones being the best for PDT photosensitization.

We have synthesized PDT photosensitizers based on porphyrins with sugar moieties as the hydrophilic substituents. The sugar acts as a water-solubilizing moiety and tumor-targeting element due to the enhanced uptake of carbohydrates by tumor cells, which is typically demonstrated by the use of 2-[^{18}F]fluoro-2-deoxy-D-glucose for cancer diagnostics using positron emission tomography. In this case, the number and the pattern of glycosylation of the porphyrin can also affect the efficacy of the PDT action. Momenteau and Maillard et al. reported the photocytotoxicity of mono-, tris- and tetrakis-glucosylated tetraphenylporphyrins and tris- and tetrakis-glucosylated tetraphenylchlorins.[11,12] They also reported that the PDT effect of these photosensitizers depended on the substitution pattern of the sugar moiety. However, their study lacked bis-glycosylated derivatives. To the best of our knowledge, there is no systematic study on the photocytotoxicity of a 'complete set' of glycoconjuagted porphyrins like TPPS and AlPcS.

In this article, we report the synthesis and structural elucidation of a 'complete set' of glycoconjuagted porphyrins, namely perfluorophenylporphyrin having *S*-glucopyranosyl groups with possible five patterns (mono-, *cis*-bis-, *trans*-bis-, tris- and tetrakis-substituted). The effect of the glycosylation pattern on the PDT action is discussed on the basis of photophysical properties as well as cellular uptake and photocytotoxicity in HeLa cells.

2. Results and discussion

2.1. Synthesis and characterization of S-glucosylated porphyrins

5,10,15,20-Tetrakis(pentafluorophenyl)porphyrin (TFPP)[13] and acetyl 2,3,4,6-tetra-*O*-acetyl-1-thio-β-D-glucopyranoside (AcSGl-

* Corresponding author. Tel.: +81 743726122; fax: +81 743726129.
E-mail address: hirohara@ms.naist.jp (S. Hirohara).

0968-0896/$ - see front matter © 2010 Elsevier Ltd. All rights reserved.
doi:10.1016/j.bmc.2010.01.006

cAc)[14] were prepared according to the literature methods. Nucleophilic substitution of TFPP by AcSGlcAc was carried out in DMF in the presence of diethylamine at ambient temperature to yield S-glycosylated porphyrins (Scheme 1). Fortunately, all five possible derivatives, namely $\mathbf{1}_{Ac}$, *cis*-$\mathbf{2}_{Ac}$, *trans*-$\mathbf{2}_{Ac}$, $\mathbf{3}_{Ac}$ and $\mathbf{4}_{Ac}$, could be separated by normal-phase high-performance liquid chromatography (HPLC) using silica gel as a stationary phase and a mixture of CH_2Cl_2 and ethyl acetate (7/3, v/v) as the eluent. Additionally, conventional preparative column chromatography was suitable for separation of the five derivatives. Figure 1 shows a representative HPLC trace of the reaction mixture using 2 equiv AcSGlcAs relative to TFPP. The degree of S-glycosylation in TFPP was easily determined by ^{1}H NMR spectroscopy. The β-pyrrole peak was strongly shifted toward the lower field by S-glycosylation of the vicinal pentafluorophenyl group (Fig. 2). As expected, the degree of S-glycosylation increased in relation to the retention time in normal-phase HPLC. The third (peak b) and fourth peaks (peak c) in the HPLC trace (Fig. 1) both indicated doubly substituted derivatives, namely *cis*-$\mathbf{2}_{Ac}$ or *trans*-$\mathbf{2}_{Ac}$, and could not be distinguished by their ^{1}H NMR spectra in $CDCl_3$. Because of the anisotropic effect of benzene, these two peaks showed clearly distinguishable ^{1}H NMR spectra in C_6D_6. The third peak (peak b) showed only two doublet peaks at 9.10 and 8.68 ppm, and the fourth (peak c) showed two singlet peaks at 9.01 and 8.70 ppm and two doublet peaks at 9.11 and 8.68 ppm in the β-pyrrole region (Fig. 3). These patterns clearly indicated that the third peak (peak b) was *trans*-$\mathbf{2}_{Ac}$ and that the fourth (peak c) was *cis*-$\mathbf{2}_{Ac}$ in normal-phase HPLC. Thus, we completely assigned the five possible TFPP derivatives having *S*-glucopyranosyl groups on the peripheral phenyl rings.

The degree of S-glycosylation could be controlled by the ratio of AcSGlcAc to TFPP in the feed (Fig. 4). By optimizing the reaction conditions and purification procedure, we obtained $\mathbf{1}_{Ac}$ (41.7%), *cis*-$\mathbf{2}_{Ac}$ (18.5%), *trans*-$\mathbf{2}_{Ac}$ (13.5%), $\mathbf{3}_{Ac}$ (31.5%) and $\mathbf{4}_{Ac}$ (82.5%) in purities of >98.5% evaluated by HPLC using a silica gel column. The saponification of S-glucosylated porphyrins $\mathbf{1}_{Ac}$, *cis*-$\mathbf{2}_{Ac}$, *trans*-$\mathbf{2}_{Ac}$, $\mathbf{3}_{Ac}$ and $\mathbf{4}_{Ac}$ was carried out using sodium methoxide in a mixture of CH_3OH and CH_2Cl_2. The crude product was purified with Bio-Beads® S-X3 and preparative column chromatography and octadecylsilyl-bound silica gel using a mixture of CH_3CN and H_2O (7/3–1/1, v/v) as the eluent. S-Glucosylated porphyrins $\mathbf{1}_{OH}$, *cis*-$\mathbf{2}_{OH}$, *trans*-$\mathbf{2}_{OH}$, $\mathbf{3}_{OH}$ and $\mathbf{4}_{OH}$ were obtained in yields of 50.9–60.9% with the purities of >97% as evaluated by HPLC using octadecylsilyl-bound silica gel. All compounds were fully characterized by means of elemental analysis, ^{1}H, ^{13}C and ^{19}F NMR and UV–vis spectroscopy.

All S-glucosylated porphyrins showed phyllo-type UV–vis spectra with absorption maximum at ca. 415 nm in the Soret region

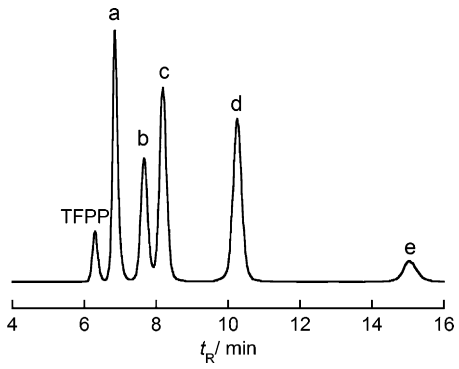

Figure 1. HPLC trace of the reaction mixture of TFPP and AcSGlcAc ($[AcGlcSAc]_0/[TFPP]_0 = 2$) recorded by UV–vis detector (413 nm). HPLC condition is described in Section 4.

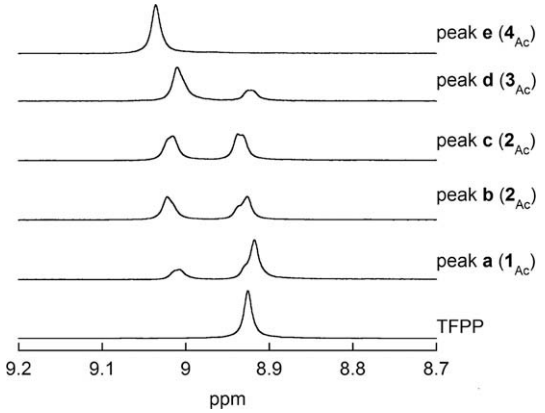

Figure 2. ^{1}H NMR spectra of β-pyrrole region of each peaks on HPLC in $CDCl_3$.

and four maxima in the Q region (from 505 to 580 nm) in DMSO. The intensity of the Q_I band decreased with an increase in the number of *S*-glucopyranosyl groups and became close to that of TFPP. On the other hand, UV–vis spectra recorded in PBS solution containing 1 vol % DMSO were different from those recorded in DMSO (Fig. 5). The spectra of S-glucosylated porphyrins $\mathbf{1}_{OH}$, *cis*-$\mathbf{2}_{OH}$, $\mathbf{3}_{OH}$ and $\mathbf{4}_{OH}$ were shifted toward shorter wavelengths in comparison with those recorded in DMSO, while the spectrum of *trans*-$\mathbf{2}_{OH}$ was shifted toward longer wavelengths. This also reflects the oscillator strength in the region over 500 nm ($f_{>500\ nm}$) listed in Table 1. In DMSO, the $f_{>500\ nm}$ values were almost independent of

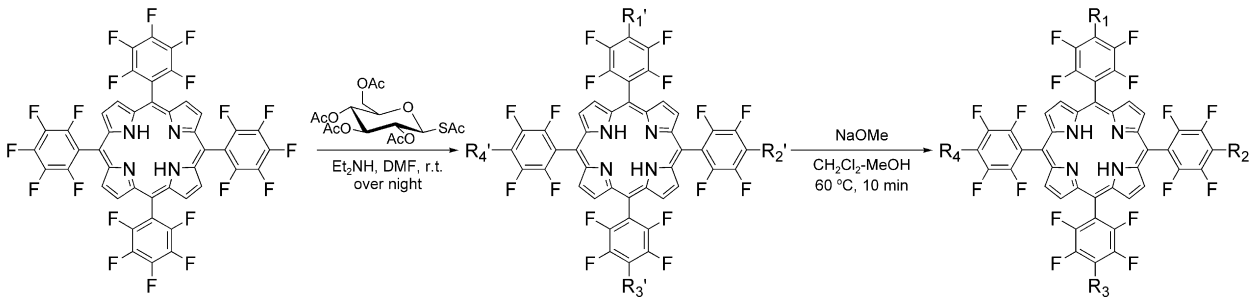

$\mathbf{1}_{Ac}$: $R_2' = R_3' = R_4' = F$; $R_2' = AcGlcS-$
cis-$\mathbf{2}_{Ac}$: $R_3' = R_4' = F$; $R_2' = R_3' = AcGlcS-$
trans-$\mathbf{2}_{Ac}$: $R_2' = R_4' = F$; $R_1' = R_3' = AcGlcS-$
$\mathbf{3}_{Ac}$: $R_4' = F$; $R_1' = R_2' = R_3' = AcGlcS-$
$\mathbf{4}_{Ac}$: $R_1' = R_2' = R_3' = R_4' = AcGlcS-$

$\mathbf{1}_{OH}$: $R_2 = R_3 = R_4 = F$; $R_1 = GlcS-$
cis-$\mathbf{2}_{OH}$: $R_3 = R_4 = F$; $R_1 = R_2 = GlcS-$
trans-$\mathbf{2}_{OH}$: $R_2 = R_4 = F$; $R_1 = R_3 = GlcS-$
$\mathbf{3}_{OH}$: $R_4 = F$; $R_1 = R_2 = R_3 = GlcS-$
$\mathbf{4}_{OH}$: $R_1 = R_2 = R_3 = R_4 = GlcS-$

Scheme 1.

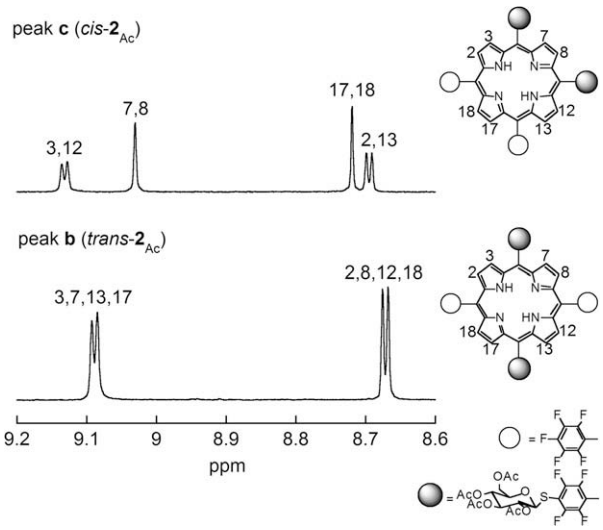

Figure 3. ^{1}H NMR spectra of β-pyrrole region of the peak **b** and peak **c** on HPLC in C_6D_6.

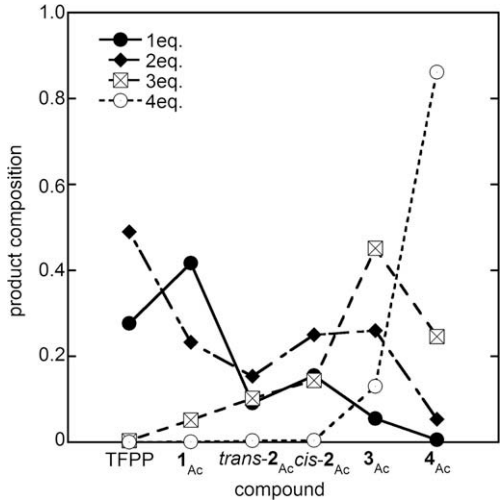

Figure 4. Molar compositions of each S-glucosylated porphyrin in the product as a function of the ratio of $[AcGlcSAc]_0/[TFPP]_0$ in the feed.

the number of *S*-glucopyranosyl groups. On the other hand, the $f_{>500\ nm}$ value increased in the order $\mathbf{4}_{OH} < \mathbf{1}_{OH}$, *cis*-$\mathbf{2}_{OH} < \mathbf{3}_{OH} <$ *trans*-$\mathbf{2}_{OH}$ in PBS solution containing 1 vol % DMSO. The $f_{>500\ nm}$ value of *trans*-$\mathbf{2}_{OH}$ was almost 1.5-fold higher than those of the other S-glycosylated porphyrins.

Upon photoabsorption of photosensitizers, two types of photoreactions with oxygen may occur to generate reactive oxygen species (ROS). One is electron transfer (type I reaction) to generate superoxide anion, hydroxyl radical, etc., and the other is energy transfer (type II reaction) to generate singlet oxygen ($^1O_2$). Among them, $^1O_2$ is usually thought to be the dominant cytotoxic species because of its relatively long lifetime. The ROS generation of S-glycosylated porphyrins $\mathbf{1}_{OH}$, *cis*-$\mathbf{2}_{OH}$, *trans*-$\mathbf{2}_{OH}$, $\mathbf{3}_{OH}$ and $\mathbf{4}_{OH}$ was studied by two methods using 1,3-diphenylisobenzofuran (DPBF) or 2,7-dichlorofluorescein diacetate (DCFDA). The DPBF-detectable ROS is mainly $^1O_2$ generated by a type II reaction, while the DCFDA-detectable ROS is radical species generated by type I reactions.

The rate constant of $^1O_2$ generation was evaluated through the degradation of DPBF upon photoirradiation of over 500 nm in wavelength in the presence of photosensitizers in DMSO saturated with O_2. The obtained rate constant was divided by the $f_{>500\ nm}$ value and normalized to the value for $\mathbf{4}_{OH}$ to give the relative efficiency of $^1O_2$ generation ($\Phi_\Delta/f_{>500\ nm}$) (Table 2). The $\Phi_\Delta/f_{>500\ nm}$ values were almost independent of the number of *S*-glucopyranosyl groups. Hence no differences were found in type II reactions between S-glucosylated porphyrins.

The production efficiency of ROS generated by type I reactions was evaluated by the initial rate of DCFDA fluorescence upon photoirradiation of over 500 nm in wavelength in the presence of photosensitizers in PBS solution containing 3% DMSO that was aerated. The obtained initial rate was divided by the $f_{>500\ nm}$ value and normalized to the value for $\mathbf{4}_{OH}$ to give the relative efficiency of DCFDA-detectable ROS production via type I reaction ($\Phi_{DCFDA}/f_{>500\ nm}$). Interestingly, the $\Phi_{DCFDA}/f_{>500\ nm}$ values were affected by the S-glycosylation pattern, and increased in the order of *cis*-$\mathbf{2}_{OH} < \mathbf{4}_{OH} < \mathbf{3}_{OH} <$ *trans*-$\mathbf{2}_{OH} < \mathbf{1}_{OH}$. Even though the details of type I photoreactions are unclear, the differences in the $\Phi_{DCFDA}/f_{>500\ nm}$ values suggest that the S-glycosylation pattern affects the efficiency of type I photoreactions.

The hydrophobicity parameter (Log *P*) is thought to be an important parameter that is closely connected to the cellular uptake behavior.[15–18] The Log *P* values of S-glucosylated porphyrins $\mathbf{1}_{OH}$, *cis*-$\mathbf{2}_{OH}$, *trans*-$\mathbf{2}_{OH}$, $\mathbf{3}_{OH}$ and $\mathbf{4}_{OH}$ were determined by reverse-phase thin layer chromatography (RP-TLC)[19,20] (Table 3). Benzaldehyde,[21] benzophenone,[22] *m*-hydroxybenzaldehyde,[23] *p*-fluorobenzaldehyde[23] and *m*-fluorobenzaldehyde[23] were used as standards for calibration. The Log *P* values of S-glucosylated porphyrins $\mathbf{1}_{OH}$, *cis*-$\mathbf{2}_{OH}$, *trans*-$\mathbf{2}_{OH}$, $\mathbf{3}_{OH}$ and $\mathbf{4}_{OH}$ were determined on the basis of the calibration (Table 3). The Log *P* value decreased from +5.1 to +0.8 in the order of $\mathbf{1}_{OH}$ > *cis*-$\mathbf{2}_{OH}$ > *trans*-$\mathbf{2}_{OH}$ > $\mathbf{3}_{OH}$ > $\mathbf{4}_{OH}$.

2.2. In vitro photocytotoxicity test of S-glucosylated porphyrins

The cytotoxicity of the five S-glucosylated porphyrins $\mathbf{1}_{OH}$, *cis*-$\mathbf{2}_{OH}$, *trans*-$\mathbf{2}_{OH}$, $\mathbf{3}_{OH}$ and $\mathbf{4}_{OH}$ and TPPS was evaluated at a concentration of 100 nM in HeLa cells with and without photoirradiation (16 J cm^{-2}). Twenty-four hours after photoirradiation, the cell survival rate was estimated in terms of the mitochondrial activity of NADH dehydrogenase using WST-8® reagent from Cell Counting Kit-8, and normalized to that of no drug treatment. Figure 6a shows the percentage of cell survival after 24 h of incubation without photoirradiation. No S-glucosylated porphyrins showed cytotoxicity in the dark. The photocytotoxicity of S-glucosylated porphyrins $\mathbf{1}_{OH}$, *cis*-$\mathbf{2}_{OH}$, *trans*-$\mathbf{2}_{OH}$, $\mathbf{3}_{OH}$ and $\mathbf{4}_{OH}$ was significantly higher than that of TPPS (Fig. 6b). In particular, S-glucosylated porphyrins $\mathbf{1}_{OH}$, *cis*-$\mathbf{2}_{OH}$, *trans*-$\mathbf{2}_{OH}$ and $\mathbf{3}_{OH}$ completely killed HeLa cells at 100 nM. Figure 7 shows the cell survival rate of S-glucosylated porphyrins $\mathbf{1}_{OH}$, *cis*-$\mathbf{2}_{OH}$, *trans*-$\mathbf{2}_{OH}$, $\mathbf{3}_{OH}$ and $\mathbf{4}_{OH}$ and TPPS in the concentration range from 100 to 1 nM. The concentrations inducing 50% cell death (EC_{50}) were estimated to be <5 nM (*trans*-$\mathbf{2}_{OH}$), ca. 80 nM ($\mathbf{3}_{OH}$) and ca. 90 nM ($\mathbf{1}_{OH}$, *cis*-$\mathbf{2}_{OH}$, $\mathbf{4}_{OH}$). Interestingly, *trans*-$\mathbf{2}_{OH}$ showed outstanding photocytotoxicity, indicating almost 20-fold higher efficacy than other S-glucosylated porphyrins. The very high photocytotoxicity of *trans*-$\mathbf{2}_{OH}$ may be partly attributable to the greater $f_{>500\ nm}$ and $\Phi_{DCFDA}/f_{>500\ nm}$ values in PBS solution; however, this is not enough to rationalize such strong photocytotoxicity.

In order to explore the mode of cell death, the morphological change induced by photoirradiation in the presence of *trans*-$\mathbf{2}_{OH}$ were examined. Figure 8 shows bright field and fluorescence images of DAPI-stained HeLa cells 3 h after photoirradiation in the presence of *trans*-$\mathbf{2}_{OH}$. Following photoirradiation, a majority of HeLa cells treated with *trans*-$\mathbf{2}_{OH}$ appeared shrunken, and numerous apoptotic bodies were formed within 3 h. Almost all of the cells treated with *trans*-$\mathbf{2}_{OH}$ were destroyed and strong

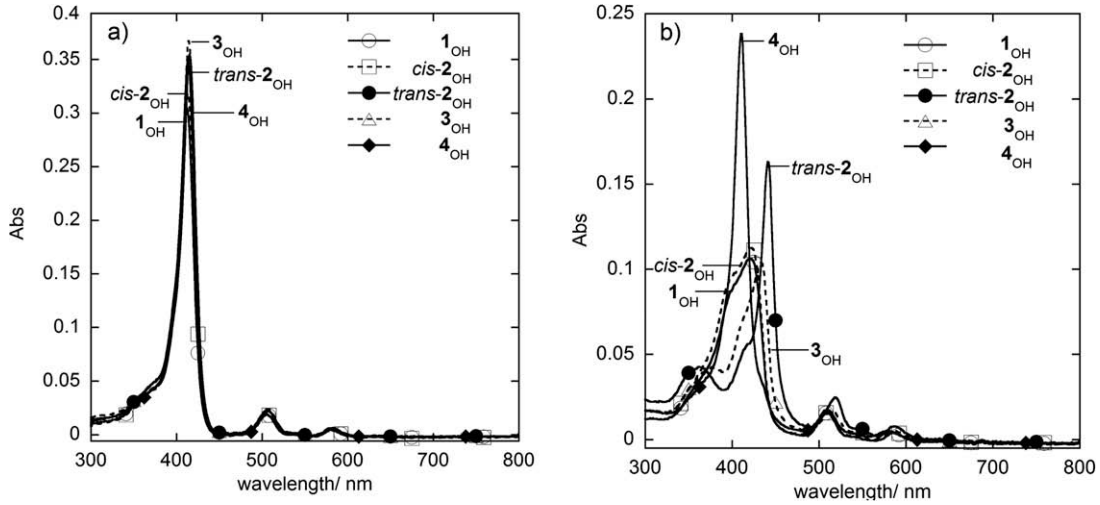

Figure 5. UV–vis spectra of S-glucosylated porphyrins $\mathbf{1}_{OH}$, *cis*-$\mathbf{2}_{OH}$, *trans*-$\mathbf{2}_{OH}$, $\mathbf{3}_{OH}$ and $\mathbf{4}_{OH}$ in DMSO: (a) and in PBS solution containing 1% DMSO; (b) at 25 °C. [Photosensitizer] = 1.0 μM.

Table 1
Oscillator strength $f_{>500\ nm}$ of S-glucosylated porphyrins $\mathbf{1}_{OH}$, *cis*-$\mathbf{2}_{OH}$, *trans*-$\mathbf{2}_{OH}$, $\mathbf{3}_{OH}$ and $\mathbf{4}_{OH}$ in DMSO and in PBS solution containing 1% DMSO at 25 °C

	$f_{>500\ nm}$[a]	
	In DMSO	In PBS solution containing 1% DMSO
$\mathbf{1}_{OH}$	0.036	0.041
cis-$\mathbf{2}_{OH}$	0.038	0.042
trans-$\mathbf{2}_{OH}$	0.044	0.071
$\mathbf{3}_{OH}$	0.048	0.051
$\mathbf{4}_{OH}$	0.044	0.026

[a] Oscillator strength in the range above 500 nm estimated as $4.32 \times 10^{-9} \int \varepsilon(\nu) d\nu$.

Table 2
Relative generation efficiency of DPBF-detectable ROS ($^1O_2$) (Φ_Δ) and DCFDA-detectable ROS (Φ_{DCFDA}) of S-glucosylated porphyrins $\mathbf{1}_{OH}$, *cis*-$\mathbf{2}_{OH}$, *trans*-$\mathbf{2}_{OH}$, $\mathbf{3}_{OH}$ and $\mathbf{4}_{OH}$

	$\Phi_\Delta/f_{>500\ nm}$[a]	$\Phi_{DCFDA}/f_{>500\ nm}$[b]
$\mathbf{1}_{OH}$	0.9	2.3
cis-$\mathbf{2}_{OH}$	1.0	0.6
trans-$\mathbf{2}_{OH}$	0.9	2.1
$\mathbf{3}_{OH}$	0.8	1.4
$\mathbf{4}_{OH}$	1.0	1.0

[a] The $\Phi_\Delta/f_{>500\ nm}$ value was evaluated by the degradation rate of DPBF by photosensitizers in DMSO under O_2 saturated condition at 37 °C, and normalized to the value for S-glucosylated porphyrin $\mathbf{4}_{OH}$.

[b] The $\Phi_{DCFDA}/f_{>500\ nm}$ value was evaluated by the initial rate of DCFDA fluorescence intensity increments by the photoirradiation in the presence of photosensitizers in PBS solution containing 3% DMSO under aerated condition at 37 °C, and normalized to the value for S-glycosylated porphyrin $\mathbf{4}_{OH}$.

Table 3
Capacity factor (R_f) in RP-TLC and hydrophobicity parameter (Log *P*) of S-glucosylated porphyrins $\mathbf{1}_{OH}$, *cis*-$\mathbf{2}_{OH}$, *trans*-$\mathbf{2}_{OH}$, $\mathbf{3}_{OH}$ and $\mathbf{4}_{OH}$

	R_f	Log k'[a]	Log P[b]
$\mathbf{1}_{OH}$	0.19	1.33	5.11
cis-$\mathbf{2}_{OH}$	0.43	0.05	3.98
trans-$\mathbf{2}_{OH}$	0.55	−0.46	3.53
$\mathbf{3}_{OH}$	0.67	−1.07	2.99
$\mathbf{4}_{OH}$	0.87	−3.61	0.75

[a] $k' = 1/R_f$.

[b] Log P = 0.886 × Log k' + 3.937.

fluorescence from DAPI was observed, suggesting an enhancement of cell membrane permeation. The morphological changes of HeLa cells induced by *trans*-$\mathbf{2}_{OH}$ and photoirradiation are characteristic of apoptotic cell death, which is the usual case in glycoconjugated photosensitizers. Therefore, no significant morphological differences were found in the mode of cell death.

2.3. In vitro study on the relationship between cellular uptake and photocytotoxicity

In the case of TPPS derivatives ($TPPS_1$, $TPPS_{cis2}$, $TPPS_{trans2}$, $TPPS_3$ and $TPPS_4$) and AlPcS derivatives ($AlPcS_1$, $AlPcS_{cis2}$, $AlPcS_{trans2}$, $AlPcS_3$ and $AlPcS_4$), the Kessel and MacDonald groups reported that the photocytotoxicity of these photosensitizers varied with the sulfonate-substitution pattern and were closely correlated with the cellular uptake rate. The cellular uptake of the five S-glucosylated porphyrins $\mathbf{1}_{OH}$, *cis*-$\mathbf{2}_{OH}$, *trans*-$\mathbf{2}_{OH}$, $\mathbf{3}_{OH}$ and $\mathbf{4}_{OH}$ by HeLa cells was examined after 24 h of incubation at a concentration of 80 nM. Figure 9 shows the relative values of the cellular uptake of S-glucosylated porphyrins $\mathbf{1}_{OH}$, *cis*-$\mathbf{2}_{OH}$, *trans*-$\mathbf{2}_{OH}$, $\mathbf{3}_{OH}$ and $\mathbf{4}_{OH}$ normalized to that of TPPS as a function of the Log *P* values. All S-glucosylated porphyrins showed higher uptake than that of TPPS. In general, a significant lipophilicity is required to interact with the hydrophobic cell membrane and pass through it, that is, to show effective cellular uptake.[15–18] In contrast, our results indicated that there is an optimum Log *P* value at ca. 3.5 for enhanced cellular uptake. The order of the cellular uptake was determined to be *trans*-$\mathbf{2}_{OH}$ > *cis*-$\mathbf{2}_{OH}$, $\mathbf{3}_{OH}$ > $\mathbf{1}_{OH}$, $\mathbf{4}_{OH}$. S-Glucosylated porphyrin *trans*-$\mathbf{2}_{OH}$ showed an uptake that was threefold greater than those of the other S-glucosylated porphyrins. Figure 10 clearly shows that the photocytotoxicity of S-glucosylated porphyrins closely correlated with the cellular uptake, as in the TPPS and AlPcS series. However, the order of photocytotoxicity and cellular uptake was different from that of the TPPS and AlPcS series. For our S-glucosylated porphyrins, TFPP with two *S*-glucopyranosyl groups at the *trans* positions was the most effective, while the porphyrin with two sulfonyl groups at the *cis* positions was the most effective in the TPPS and AlPcS series.

Based on of the EC_{50} values, S-glucosylated porphyrin *trans*-$\mathbf{2}_{OH}$ exerted almost 20-fold higher photocytotoxicity compared with other S-glucosylated porphyrins $\mathbf{1}_{OH}$, *cis*-$\mathbf{2}_{OH}$, $\mathbf{3}_{OH}$ and $\mathbf{4}_{OH}$. This very high photocytotoxicity of *trans*-$\mathbf{2}_{OH}$ is irrefutable and relates to the several factors, namely (1) high optical transition probability

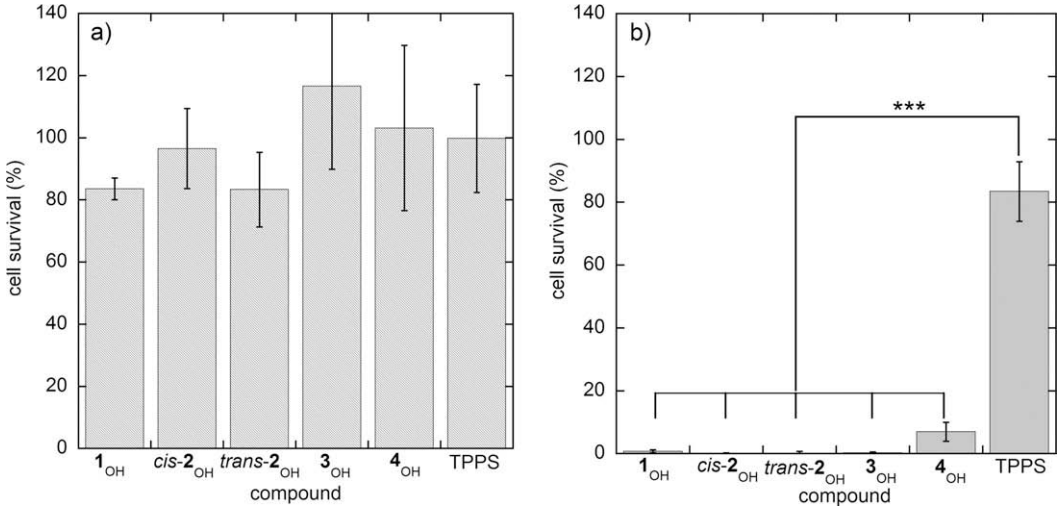

Figure 6. Dark (a) and photocytotoxicity (b) of S-glucosylated porphyrins $\mathbf{1}_{OH}$, *cis*-$\mathbf{2}_{OH}$, *trans*-$\mathbf{2}_{OH}$, $\mathbf{3}_{OH}$, $\mathbf{4}_{OH}$ and TPPS in HeLa cells. [Photosensitizers] = 100 nM. The light dose was 16 J cm^{-2} from a 100 W halogen lamp (λ >500 nm). Values are the mean ± standard deviation of six replicate experiments. *** Significant difference, p <0.001.

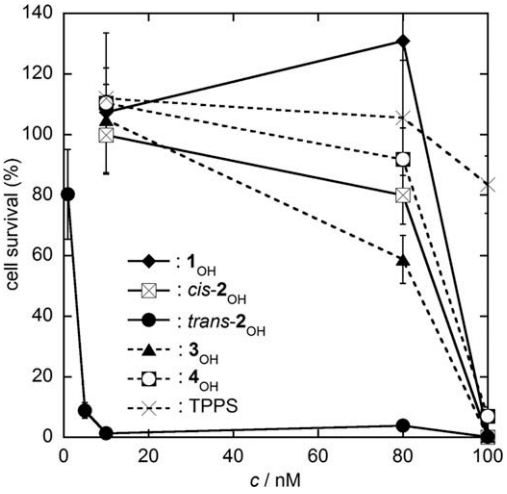

Figure 7. Plots of cell survival rate (%) of HeLa cells treated with S-glucosylated porphyrins $\mathbf{1}_{OH}$, *cis*-$\mathbf{2}_{OH}$, *trans*-$\mathbf{2}_{OH}$, $\mathbf{3}_{OH}$, $\mathbf{4}_{OH}$ and TPPS as a function of the photosensitizer concentration. The light dose was 16 J cm^{-2} from a 100 W halogen lamp (λ >500 nm). Values are the mean ± standard deviation of six replicate experiments.

in aqueous media (the $f_{>500\ nm}$ value), (2) high efficiency of type I photoreaction (the $\Phi_{DCFDA}/f_{>500\ nm}$ value) and (3) enhanced cellular uptake. A study on the detailed mechanism of the outstanding photocytotoxity of S-glucosylated porphyrin *trans*-$\mathbf{2}_{OH}$ is in progress in our laboratory.

3. Conclusion

We synthesized five possible TFPP derivatives having *S*-glucopyranosyl groups (mono-, *cis*-bis-, *trans*-bis-, tris- and tetrakis-substituted) and made an indubitable structural assignment. Both the cellular uptake and the photocytotoxicity of *trans*-$\mathbf{2}_{OH}$ in HeLa cells were extremely high compared with other S-glucosylated porphyrins $\mathbf{1}_{OH}$, *cis*-$\mathbf{2}_{OH}$, $\mathbf{3}_{OH}$ and $\mathbf{4}_{OH}$. The superiority of *trans*-$\mathbf{2}_{OH}$ is attributable to several factors such as high optical transition probability in aqueous solution, efficient type I photoreactions and enhanced cellular uptake. Therefore, hydrophobic photosensitizing dyes having sugar moieties at the *trans*-positions are a promising scaffold for PDT photosensitizers.

4. Experimental

4.1. Measurements

Preparative gel permeation chromatography (GPC) was performed on LC-908 recycling preparative high-performance liquid chromatography (HPLC) system (Japan Analytical Industry Co., Ltd, Japan) equipped with two polystyrene columns (JAIGEL-2.5H and JAIGEL-2H), with $CHCl_3$ as an eluent. Preparative HPLC was carried out using octadecylsilyl-bound silica gel (Mightysil RP-18, 20 mmϕ × 250 mm, KANTO CHEMICAL Co., Inc., Tokyo, Japan). The purity of the porphyrins was determined by high-performance liquid chromatography (HPLC, Waters, 1515 Isocratic HPLC, Waters corp.) equipped with silica gel (COSMOSIL 5SL-II Packed Column, 4.6 mmϕ × 150 mm, Nacalai tesque. Inc., Kyoto, Japan) and octadecylsilyl-bonded silica gel (Mightysil RP-18, 4.6 mmϕ × 250 mm, KANTO CHEMICAL Co., Inc., Tokyo, Japan) column and a UV–vis detector (Waters, 2487 Dual l Absorbance Detector). Elemental analysis was carried out using a Perkin–Elmer PE2400 Series II CHNS/O Analyzer (PerkinElmer Co., Ltd, Shelton, CT). ^{1}H, ^{13}C and ^{19}F NMR spectra were recorded using JNM-EC600 (600 MHz, JEOL Ltd, Tokyo, Japan) instruments. UV–vis spectra were recorded on a V-570 spectrophotometer (JASCO Co., Ltd, Tokyo, Japan). Steady-state fluorescence (FL) spectra were recorded on FP-6300 spectrofluorometer (JASCO Co., Ltd, Tokyo, Japan). Stock solutions of photosensitizers were prepared by weighing the dried photosensitizers and dissolving them in dimethyl sulfoxide (DMSO, Wako Pure Chemical Industries, Osaka, Japan), and kept in freezer (−30 °C) until use. Absorbance and fluorescence intensity of wells were determined with plate readers (Multiscan JX, Thermo Fisher Scientific Co., Yokohama, Japan and SPECTRA Fluor Plus, TECAN Group Ltd, Seestrasse, Switzerland, respectively). Bright field and fluorescence images of cells were taken by using a confocal laser scanning microscope (CLSM, Model LSM 510, Carl Zeiss, Jena, Germany).

4.2. Materials

4.2.1. General chemicals

All chemicals were of analytical grade. Tetraphenylporphyrin tetrasulfonic acid (TPPS) and 1,3-diphenylisobenzofuran (DPBF) was purchased from Sigma–Aldrich Japan (Chiba, Japan). 4′,6-Diamidino-2-phenylindole dihydrochloride hydrate (DAPI) and

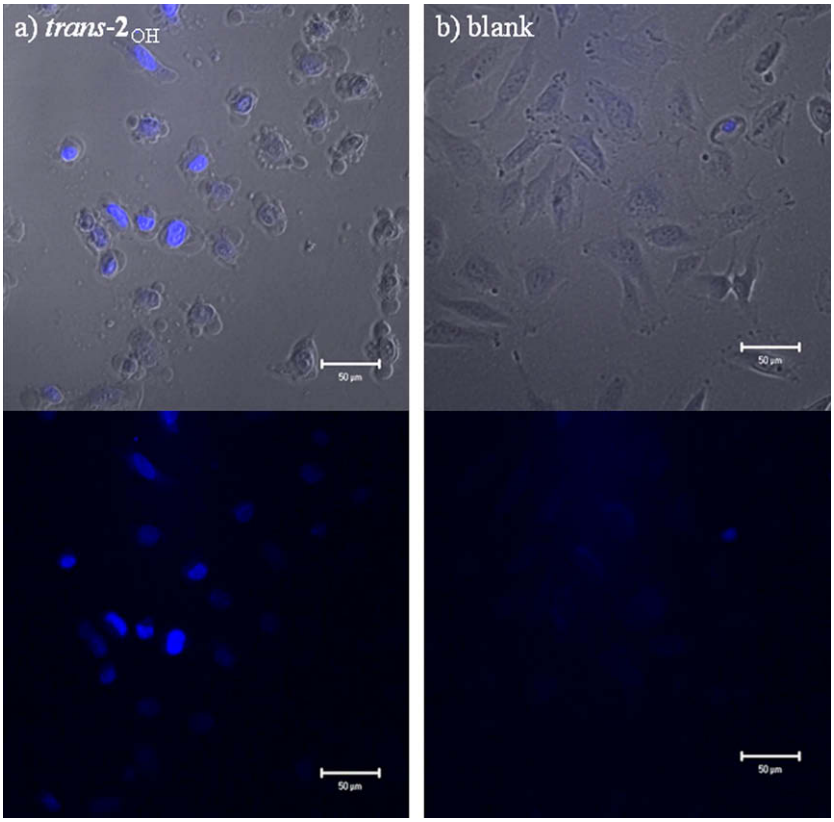

Figure 8. Bright field (upper) and fluorescence (lower) images of DAPI-stained HeLa cells treated with S-glucosylated porphyrin *trans*-$\mathbf{2}_{OH}$ (a) and blank (b) at 3 h after photoirradiation. [*trans*-$\mathbf{2}_{OH}$] = 500 nM. Excitation wavelength was 364 nm.

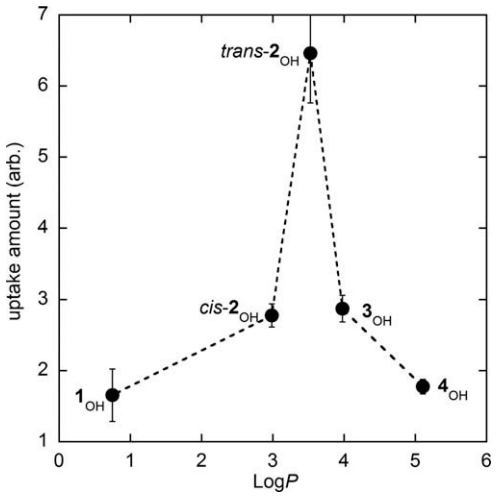

Figure 9. Plot of the relative cellular uptake amount (arb.) of S-glucosylated porphyrins $\mathbf{1}_{OH}$, *cis*-$\mathbf{2}_{OH}$, *trans*-$\mathbf{2}_{OH}$, $\mathbf{3}_{OH}$ and $\mathbf{4}_{OH}$ by HeLa cells as a function of Log *P* value. Values are the mean ± standard deviation of three replicate experiments.

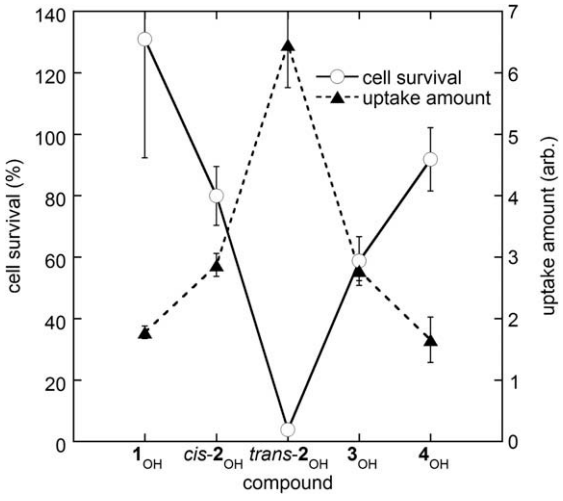

Figure 10. Cell survival rate (%) of HeLa cells treated with S-glucosylated porphyrins ([photosensitizer] = 80 nM, light dose was 16 J cm^{-2}, λ >500 nm) and relative cellular uptake amount (arb.) of S-glycosylated porphyrins by HeLa cells. Values are the mean ± standard deviation of three (for cellular uptake) and six (for photocytotoxicity) replicate experiments.

2,7-dichlorofluorescein diacetate (DCFDA) were purchased from Molecular Probes (Eugene, OR). 5,10,15,20-Tetrakis(pentafluorophenyl)porphyrin (TFPP)[13], acetyl 2,3,4,6-tetra-*O*-acetyl-1-thio-β-D-glucopyranoside (AcGlcSAc),[14] 5,10,15,20-tetrakis[4-(2,3,4,6-tetra-*O*-acetyl-β-D-glucopyranosylthio)-2,3,5,6-tetrafluorophenyl)]porphyrin ($\mathbf{4}_{Ac}$)[24] and 5,10,15,20-tetrakis[4-(β-D-glucopyranosylthio)-2,3,5,6-tetrafluorophenyl)]porphyrin ($\mathbf{4}_{OH}$)[24] were prepared according to the literature.

4.2.2. 5-[4-(2,3,4,6-Tetra-*O*-acetyl-β-d-glucopyranosylthio)-2,3,5,6-tetrafluorophenyl)]-10,15,20-tris(2,3,4,5,6-pentafluorophenyl)porphyrin ($\mathbf{1}_{Ac}$)

TFPP (49.3 mg, 50.6 μmol), AcGlcSAc (20.9 mg, 51.5 μmol) and diethylamine (37 μL, 724 μmol) were dissolved in DMF (10 mL). The reaction mixture was stirred at room temperature for 24 h, diluted with $CHCl_3$ (15 mL) and washed with distilled water

(15 mL × 5). The extract was dried over Na_2SO_4, and the solvent was removed under reduced pressure. The crude product was purified by column chromatography (silica gel, CH_2Cl_2 to CH_2Cl_2/AcOEt = 100–60:40) followed by preparative GPC to give **1_{Ac}** (28.0 mg, yield 41.7%) as a brownish purple solid. Purity (HPLC): 98.7%. Anal. Calcd for $C_{58}H_{29}O_9N_4F_{19}S_1 + H_2O$: C, 52.11; H, 2.34; N, 4.19. Found: C, 52.31; H, 2.19; N, 4.88. ^{1}H NMR (600.17 MHz, $CDCl_3$, Si(CH_3)$_4$ = 0 ppm): δ (ppm) = 9.01 (2H, br s, 3,7-β-pyrrole*H*), 8.92 (6H, br s, 2,8,12,13,17,18-β-pyrrole*H*), 5.38 (1H, dd, ^3J = 9.2 Hz and 9.2 Hz, 3′-Glc*H*), 5.24 (2H, m, 2′,4′-Glc*H*), 5.17 (1H, d, ^3J = 10.0 Hz, 1′-Glc*H*), 4.32 (2H, m, 6′-Glc*H*), 3.90 (1H, m, 5′-Glc*H*), 2.23 (3H, s, CH_3), 2.10 (3H, s, CH_3), 2.09 (3H, s, CH_3), 2.07 (3H, s, CH_3), −2.89 (2H, br s, N*H*). ^{13}C NMR ($CDCl_3$, 100.40 MHz, *C*DCl_3 = 77 ppm): δ (ppm) = 170.63 (*C*═O), 170.16 (*C*═O), 169.46 (*C*═O), 169.39 (*C*═O), 147.90–145.39 (2,6-Ph*C*, 3,5-Ph*C*, α-pyrrole*C*), 131.12 (β-pyrrole*C*), 122.04 (4-Ph*C*), 111.85 (1-Ph*C*), 104.27 (meso*C*), 84.42 (1′-Glc*C*), 76.40 (5′-Glc*C*), 73.89 (3′-Glc*C*), 70.60 (2′-Glc*C*), 68.06 (4′-Glc*C*), 61.78 (6′-Glc*C*), 20.61 (*C*H$_3$), 20.56 (*C*H$_3$). ^{19}F NMR (564.72 MHz, $CDCl_3$, CF_3CO_2H = −76.05 ppm): δ (ppm) = −131.97 (2F, dd, $^3J_{F-F}$ = 13.9 Hz, $^2J_{F-F}$ = 6.9 Hz, 3,5-Ph*F*Glc), −136.43 (2F, dd, $^3J_{F-F}$ = 13.9 Hz, $^5J_{F-F}$ = 6.9 Hz, 2,6-Ph*F* Glc), −136.88 (6F, dd, $^3J_{F-F}$ = 13.9 Hz, $^5J_{F-F}$ = 6.9 Hz, 3,5-Ph*F*), −151.63 (3F, dd, $^3J_{F-F}$ = 13.9 Hz, $^5J_{F-F}$ = 6.9 Hz, 4-Ph*F*), −161.69 (6F, dd, $^3J_{F-F}$ = 13.9 Hz, $^5J_{F-F}$ = 6.9 Hz, 2,6-Ph*F*). UV–vis (*c* = 8.35 μM, DMSO, path length = 1 cm, 25 °C): λ /nm ($\varepsilon \times 10^{-4}$/M^{-1} cm^{-1}) = 414 (29.9), 506 (2.41), 537 (0.39), 580 (0.83), 632 (0.12). FL (*c* = 8.35 μM, DMSO, path length = 1 cm, λ_{ex} = 414.5 nm, 25 °C, N_2): λ/nm = 638, 703.

4.2.3. 5,10-Bis[4-(2,3,4,6-tetra-*O*-acetyl-β-D-glucopyranosylthio)-2,3,5,6-tetrafluorophenyl)]-15,20-bis(2,3,4,5,6-pentafluorophenyl)porphyrin (*cis*-2_{Ac})

A procedure similar to that described for **1_{Ac}** was applied to TFPP (50.0 mg, 51.3 μmol) and AcGlcSAc (41.6 mg, 102.5 μmol) to give *cis*-**2_{Ac}** (15.8 mg, yield 18.5%) as a brownish purple solid. Purity (HPLC): >99%. Anal. Calcd for $C_{72}H_{48}O_{18}N_4F_{18}S_2$: C, 51.99; H, 2.91; N, 3.37. Found: C, 51.85; H, 2.94; N, 3.62. ^{1}H NMR (600.17 MHz, $CDCl_3$, Si(CH_3)$_4$ = 0 ppm): δ (ppm) = 9.02 (4H, br s, 3,7,8,12-β-pyrrole*H*), 8.93 (4H, br s, 2,13,17,18-β-pyrrole*H*), 5.38 (2H, dd, ^3J = 9.3 Hz and 9.3 Hz, 3′-Glc*H*), 5.24 (4H, dd, ^3J = 9.8 Hz and 9.8 Hz, 2′,4′-Glc*H*), 5.18 (2H, d, ^3J = 10.0 Hz, 1′-Glc*H*), 4.32 (4H, m, 6′-Glc*H*), 3.91 (2H, dt, ^3J = 9.9 Hz and 3.8 Hz, 5′-Glc*H*), 2.23 (6H, s, CH_3), 2.10 (6H, s, CH_3), 2.09 (6H, s, CH_3), 2.07 (6H, s, CH_3), −2.89 (2H, br s, N*H*). ^{1}H NMR (600.17 MHz, C_6D_6, Si(CH_3)$_4$ = 0 ppm): δ (ppm) = 9.11 (4H, d, ^3J = 4.7 Hz, 3,12-β-pyrrole*H*), 9.01 (2H, s, 7,8-β-pyrrole*H*), 8.70 (2H, s, 17,18-β-pyrrole*H*), 8.68 (2H, d, ^3J = 4.7 Hz, 2,3-β-pyrrole*H*), 5.44 (2H, dd, ^3J = 9.1 Hz and 4.7 Hz, 3′-Glc*H*), 5.42 (2H, dd, ^3J = 9.7 Hz and 5.4 Hz, 2′-Glc*H*), 5.36 (2H, dd, ^3J = 9.6 Hz and 7.0 Hz, 4′-Glc*H*), 4.74 (2H, d, ^3J = 9.3 Hz, 1′-Glc*H*), 4.26 (2H, dd, ^3J = 12.5 Hz, ^2J = 2.2 Hz, 6′-Glc*H*), 4.18 (2H, dd, ^3J = 12.6 Hz, ^2J = 4.5 Hz, 6′-Glc*H*), 3.25 (2H, ddd, ^3J = 9.9 Hz, 4.4 Hz and 2.5 Hz, 5′-Glc*H*), 1.94 (6H, s, CH_3), 1.74 (6H, s, CH_3), 1.72 (6H, s, CH_3), 1.66 (6H, s, CH_3), −3.23 (2H, br s, N*H*). ^{13}C NMR ($CDCl_3$, 100.40 MHz, *C*DCl_3 = 77 ppm): δ (ppm) = 170.65 (*C*═O), 170.19 (*C*═O), 169.48 (*C*═O), 169.41 (*C*═O), 147.94–133.17 (2,6-Ph*C*, 3,5-Ph*C*, α-pyrrole*C*), 131.75 (β-pyrrole*C*), 122.03 (4-Ph*C*), 115.58 (1-Ph*C*), 104.30, 103.63 (meso*C*), 84.43 (1′-Glc*C*), 76.46 (5′-Glc*C*), 73.95 (3′-Glc*C*), 70.63 (2′-Glc*C*), 68.10 (4′-Glc*C*), 61.82 (6′-Glc*C*), 20.64 (*C*H$_3$), 20.60 (*C*H$_3$). ^{19}F NMR (564.72 MHz, $CDCl_3$, CF_3CO_2H = −76.05 ppm): δ (ppm) = −132.07 (4F, dd, $^3J_{F-F}$ = 13.9 Hz, $^5J_{F-F}$ = 6.9 Hz, 3,5-Ph*F*Glc), −136.41 (4F, dd, $^3J_{F-F}$ = 13.9 Hz, $^5J_{F-F}$ = 6.9 Hz, 2,6-Ph*F*Glc), −136.84 (4F, dd, $^3J_{F-F}$ = 13.9 Hz, $^5J_{F-F}$ = 6.9 Hz, 3,5-Ph*F*, −151.64 (2F, dd, $^3J_{F-F}$ = 20.8 Hz, 4-Ph*F*), −161.71 (4F, dd, $^3J_{F-F}$ = 13.9 Hz, $^5J_{F-F}$ = 6.9 Hz, 2,6-Ph*F*). UV–vis (*c* = 8.35 μM, DMSO, path length = 1 cm, 25 °C): λ /nm ($\varepsilon \times 10^{-4}$/M^{-1} cm^{-1}) = 414 (30.3), 507 (2.35), 537 (0.39), 581 (0.79), 633 (0.10). FL (*c* = 8.06 μM, DMSO, path length = 1 cm, λ_{ex} = 413 nm, 25 °C, N_2): λ/nm = 639, 703.

4.2.4. 5,15-Bis[4-(2,3,4,6-tetra-*O*-acetyl-β-D-glucopyranosylthio)-2,3,5,6-tetrafluorophenyl)]-10,20-bis(2,3,4,5,6-pentafluorophenyl)porphyrin (*trans*-2_{Ac})

A procedure similar to that described for **1_{Ac}** was applied to TFPP (50.0 mg, 51.3 μmol) and AcGlcSAc (41.6 mg, 102.5 μmol) to give *trans*-**2_{Ac}** (11.5 mg, yield 13.5%) as a brownish purple solid. Purity (HPLC): >99%. Anal. Calcd for $C_{72}H_{48}O_{18}N_4F_{18}S_2$: C, 51.99; H, 2.91; N, 3.37. Found: C, 52.05; H, 2.87; N, 3.66. ^{1}H NMR (600.17 MHz, $CDCl_3$, Si(CH_3)$_4$ = 0 ppm): δ (ppm) = 9.01 (4H, br s, 3,7,13,17-β-pyrrole*H*), 8.93 (4H, br s, 2,8,12,18-β-pyrrole*H*), 5.38 (2H, dd, ^3J = 9.2 Hz and 9.2 Hz, 3′-Glc*H*), 5.25 (4H, dd, ^3J = 10.0 Hz and 6.3 Hz, 2′,4′-Glc*H*), 5.18 (2H, d, ^3J = 10.0 Hz, 1′-Glc*H*), 4.32 (4H, m, 6′-Glc*H*), 3.91 (2H, dt, ^3J = 7.0 Hz and 3.2 Hz, 5′-Glc*H*), 2.23 (6H, s, CH_3), 2.10 (6H, s, CH_3), 2.09 (6H, s, CH_3), 2.07 (6H, s, CH_3), −2.89 (2H, br s, N*H*). ^{1}H NMR (600.17 MHz, C_6D_6, Si(CH_3)$_4$ = 0 ppm): δ (ppm) = 9.10 (4H, d, ^3J = 4.4 Hz, 3,7,13,17-β-pyrrole*H*), 8.68 (4H, d, ^3J = 4.7 Hz, 2,8,12,18-β-pyrrole*H*), 5.43 (2H, dd, ^3J = 9.0 Hz and 5.9 Hz, 3′-Glc*H*), 5.42 (2H, dd, ^3J = 9.7 Hz and 5.9 Hz, 2′-Glc*H*), 5.37 (2H, dd, ^3J = 9.8 Hz and 6.2 Hz, 4′-Glc*H*), 4.72 (2H, d, ^3J = 9.3 Hz, 1′-Glc*H*), 4.26 (2H, dd, ^3J = 12.6 Hz, ^2J = 2.3 Hz, 6′-Glc*H*), 4.18 (2H, dd, ^3J = 12.8 Hz, ^2J = 4.7 Hz, 6′-Glc*H*), 3.24 (2H, ddd, ^3J = 9.9 Hz, 4.7 Hz and 2.8 Hz, 5′-Glc*H*), 1.95 (6H, s, CH_3), 1.72 (6H, s, CH_3), 1.71 (6H, s, CH_3), 1.65 (6H, s, CH_3), −3.23 (2H, br s, N*H*). ^{13}C NMR ($CDCl_3$, 100.40 MHz, $CDCl_3$ = 77 ppm): δ (ppm) = 170.66 (*C*═O), 170.20 (*C*═O), 169.48 (*C*═O), 169.42 (*C*═O), 147.95–145.39 (2,6-Ph*C*, 3,5-Ph*C*), 141.43–136.71 (α-pyrrole*C*), 131.46 (β-pyrrole*C*), 122.03 (4-Ph*C*), 111.85 (1-Ph*C*), 104.31, 103.62 (meso*C*), 84.41 (1′-Glc*C*), 76.38 (5′-Glc*C*), 73.96 (3′-Glc*C*), 70.63 (2′-Glc*C*), 68.16 (4′-Glc*C*), 61.84 (6′-Glc*C*), 20.65 (CH_3), 20.61 (CH_3). 19F NMR (564.72 MHz, $CDCl_3$, CF_3CO_2H = −76.05 ppm): δ (ppm) = −131.97 (4F, dd, $^3J_{F-F}$ = 13.9 Hz, $^5J_{F-F}$ = 6.9 Hz, 3,5-Ph*F*Glc), −136.39 (4F, dd, $^3J_{F-F}$ = 13.9 Hz, $^5J_{F-F}$ = 6.9 Hz, 2,6-Ph*F*Glc), −136.85 (4F, dd, $^3J_{F-F}$ = 13.9 Hz, $^5J_{F-F}$ = 6.9 Hz, 3,5-Ph*F*), −151.65 (2F, dd, $^3J_{F-F}$ = 13.9 Hz, $^5J_{F-F}$ = 6.9 Hz, 4-Ph*F*), −161.71 (4F, dd, $^3J_{F-F}$ = 13.9 Hz, $^5J_{F-F}$ = 6.9 Hz, 2,6-Ph*F*). UV–vis (*c* = 7.94 μM, DMSO, path length = 1 cm, 25 °C): λ /nm ($\varepsilon \times 10^{-4}$/M^{-1} cm^{-1}) = 414 (30.9), 507 (2.25), 535 (0.31), 581 (0.49), 633 (0.07). FL (*c* = 7.94 μM, DMSO, path length = 1 cm, λ_{ex} = 413 nm, 25 °C, N_2): λ/nm = 640, 704.

4.2.5. 5,10,15-Tris[4-(2,3,4,6-tetra-O-acetyl-β-D-glucopyranosylthio)-2,3,5,6-tetrafluorophenyl)]-20-(2,3,4,5,6-pentafluorophenyl)porphyrin (3_{Ac})

A procedure similar to that described for **1_{Ac}** was applied to TFPP (49.5 mg, 50.8 μmol) and AcGlcSAc (61.9 mg, 152.5 μmol) to give **3_{Ac}** (32.2 mg, yield 31.5%) as a brownish purple solid. Purity (HPLC): >99%. Anal. Calcd for $C_{86}H_{70}O_{27}N_4F_{17}S_3 + 4H_2O$: C, 49.67; H, 3.63; N, 2.35. Found: C, 49.31; H, 3.13; N, 2.71. ^{1}H NMR (600.17 MHz, $CDCl_3$, Si(CH_3)$_4$ = 0 ppm): δ (ppm) = 9.01 (6H, br s, 3,7,8,12,13,17-β-pyrrole*H*), 8.93 (2H, br s, 2,18-β-pyrrole*H*), 5.38 (3H, dd, ^3J = 9.2 Hz and 9.2 Hz, 3′-Glc*H*), 5.25 (6H, dd, ^3J = 9.5 Hz and 9.5 Hz, 2′,4′-Glc*H*), 5.18 (3H, d, ^3J = 10.0 Hz, 1′-Glc*H*), 4.32 (6H, m, 6′-Glc*H*), 3.91 (3H, dt, ^3J = 10.1 Hz and 3.7 Hz, 5′-Glc*H*), 2.23 (9H, s, CH_3), 2.11 (9H, s, CH_3), 2.10 (9H, s, CH_3), 2.08 (9H, s, CH_3), −2.87 (2H, br s, N*H*). ^{13}C NMR ($CDCl_3$, 100.40 MHz, *C*DCl_3 = 77 ppm): δ (ppm) = 170.65 (*C*═O), 170.18 (*C*═O), 169.47 (*C*═O), 169.40 (*C*═O), 147.92–136.61 (2,6-Ph*C*, 3,5-Ph*C*, α-pyrrole*C*), 131.27 (β-pyrrole*C*), 122.03 (4-Ph*C*), 111.88 (1-Ph*C*), 104.27, 103.60 (meso*C*), 84.42 (1′-Glc*C*), 76.43 (5′-Glc*C*), 73.92 (3′-Glc*C*), 70.61 (2′-Glc*C*), 68.08 (4′-Glc*C*), 61.81 (6′-Glc*C*), 20.63 (*C*H$_3$), 20.58 (*C*H$_3$). ^{19}F NMR (564.72 MHz, $CDCl_3$, CF_3CO_2H = −76.05 ppm): δ (ppm) = −132.05 (6F, dd, $^3J_{F-F}$ = 13.9 Hz, $^5J_{F-F}$ = 6.9 Hz, 3,5-Ph*F*Glc), −136.33 (6F, dd, $^3J_{F-F}$ = 13.9 Hz, $^5J_{F-F}$ = 6.9 Hz, 2,6-

PhFGlc), −136.82 (2F, m, 3,5-PhF), −151.62 (1F, dd, $^3J_{F-F}$ = 13.9 Hz, $^5J_{F-F}$ = 6.9 Hz, 4-PhF), −161.72 (2F, dd, $^3J_{F-F}$ = 13.9 Hz, $^5J_{F-F}$ = 6.9 Hz, 2,6-PhF). UV–vis (c = 8.00 μM, DMSO, path length = 1 cm, 25 °C): λ/nm ($\varepsilon \times 10^{-4}/M^{-1}\,cm^{-1}$) = 414 (31.1), 507 (2.27), 534 (0.31), 581 (0.75), 633 (0.07). FL (c = 8.00 μM, DMSO, path length = 1 cm, λ_{ex} = 413 nm, 25 °C, N_2): λ/nm = 641, 704.

4.2.6. 5-[4-(β-D-Glucopyranosylthio)-2,3,5,6-tetrafluorophenyl)]-10,15,20-tris(2,3,4,5,6-pentafluorophenyl)porphyrin ($\mathbf{1_{OH}}$)

$\mathbf{1_{Ac}}$ (23.7 mg, 18.0 μmol) was dissolved in CH_2Cl_2 (20 mL) and MeOH (20 mL). Sodium methoxide (NaOMe) was added to adjust the pH to 9. This mixture was refluxed for 7 min at 45–50 °C, then neutralized with acetic acid. The solvent was removed, and the crude product was washed with distilled water (15 mL × 5). The crude product was purified by column chromatography (Cosmosil®, acetonitrile/H_2O = 8:2) and washed with distilled water to give $\mathbf{1_{OH}}$ (12.5 mg, yield 60.9%) as a brownish purple solid. Purity (HPLC): 97%. Anal. Calcd for $C_{50}H_{21}O_5N_4F_{19}S_1 + CH_3CN + 3H_2O$: C, 50.13; H, 2.43; N, 5.62. Found: C, 50.39; H, 2.16; N, 5.87. ^{1}H NMR (600.17 MHz, CD_3OD, CHD_2OD = 3.30 ppm): δ (ppm) = 9.59, 9.17 (8H, s, β-pyrroleH), 5.18 (2H, d, ^3J = 9.3 Hz, 1′-GlcH), 4.01 (1H, dd, ^3J = 12.0 Hz, ^2J = 1.7 Hz, 6′-GlcH), 3.78 (1H, dd, ^3J = 6.1 Hz, ^2J = 3.1 Hz, 6′-GlcH), 3.53–3.33 (4H, m, 2′,3′,4′,5′-GlcH). ^{13}C NMR (150.92 MHz, CD_3OD, CD_3OD = 49.0 ppm): δ (ppm) = 157.20–129.85 (α,β-pyrroleC, 2,6-PhC and 3,5-PhC), 121.70 (4-PhC), 116.70 (1-PhC), 106.10, 104.91 (mesoC), 86.79 (1′-GlcC), 82.81 (5′-GlcC), 79.77 (3′-GlcC), 75.99 (2′-GlcC), 71.76 (4′-GlcC), 63.11 (6′-GlcC). ^{19}F NMR (564.72 MHz, $CDCl_3$, CF_3CO_2H = −76.05 ppm): δ (ppm) = −132.68 (2F, dd, $^3J_{F-F}$ = 13.9 Hz, $^5J_{F-F}$ = 6.9 Hz, 3,5-PhFGlc), −137.77 (6F, m, $^3J_{F-F}$ = 20.8 Hz, 3,5-PhF), −138.18 (2F, dd, $^3J_{F-F}$ = 13.9 Hz, $^5J_{F-F}$ = 6.9 Hz, 2,6-PhFGlc), −152.99 (3F, t, $^3J_{F-F}$ = 17.3 Hz, $^5J_{F-F}$ = 6.8 Hz, 4-PhF), −162.59 (6F, dd, $^3J_{F-F}$ = 13.9 Hz, $^5J_{F-F}$ = 6.9 Hz, 2,6-PhF). UV–vis (c = 8.00 μM, DMSO, path length = 1 cm, 37 °C): λ/nm ($\varepsilon \times 10^{-4}/M^{-1}\,cm^{-1}$) = 413 (32.6), 505 (2.56), 536 (0.48), 582 (0.88), 633 (0.17). FL (c = 8.00 μM, DMSO, path length = 1 cm, λ_{ex} = 412.5 nm, 25 °C): λ/nm = 638, 704.

4.2.7. 5,10-Bis[4-(β-D-glucopyranosylthio)-2,3,5,6-tetrafluorophenyl)]-15,20-bis(2,3,4,5,6-pentafluorophenyl)porphyrin (*cis*-$\mathbf{2_{OH}}$)

A procedure similar to that described for $\mathbf{1_{OH}}$ as applied to ***cis*-$\mathbf{2_{OH}}$** (81.2 mg, 48.8 μmol). The crude product was purified by column chromatography (Cosmosil®, acetonitrile/H_2O = 6:4) and washed with distilled water to give *cis*-$\mathbf{2_{OH}}$ (35.5 mg, yield 54.9%) as a dark red powder. Purity (HPLC): 98%. Anal. Calcd for $C_{56}H_{32}O_{10}N_4F_{18}S_2 + C_2H_3N + 3H_2O$: C, 48.99; H, 2.91; N, 4.92. Found: C, 48.59; H, 2.61; N, 4.92. ^{1}H NMR (600.17 MHz, CD_3OD, CHD_2OD = 3.30 ppm): δ (ppm) = 9.29, 9.01 (8H, br s, β-pyrroleH), 5.17 (2H, d, ^3J = 9.0 Hz, 1′-GlcH), 4.00 (2H, dd, ^3J = 12.1 Hz, ^2J = 1.6 Hz, 6′-GlcH), 3.76 (2H, dd, ^3J = 6.1 Hz, ^2J = 3.1 Hz, 6′-GlcH), 3.53–3.43 (8H, m, 2′,3′,4′,5′-GlcH). ^{13}C NMR (150.92 MHz, CD_3OD, CD_3OD = 49.0 ppm): δ (ppm) = 157.33–129.56 (α,β-pyrroleC, 2,6-PhC and 3,5-PhC), 121.74 (4-PhC), 116.71, 115.23 (1-PhC), 106.04, 104.81 (mesoC), 86.75 (1′-GlcC), 82.80 (5′-GlcC), 79.77 (3′-GlcC), 75.99 (2′-GlcC), 71.75 (4″-GlcC), 63.11 (6′-GlcC). ^{19}F NMR (564.72 MHz, CD_3OD, CF_3CO_2H = −76.05 ppm): δ (ppm) = −132.58 (4F, dd, $^3J_{F-F}$ = 13.9 Hz, $^5J_{F-F}$ = 6.9 Hz, 3,5-PhFGlc), −137.66 (4F, d, $^3J_{F-F}$ = 20.8 Hz, 3,5-PhF), −138.05 (4F, dd, $^3J_{F-F}$ = 13.9 Hz, $^5J_{F-F}$ = 6.9 Hz, 2,6-PhFGlc), −152.91 (2F, dd, $^3J_{F-F}$ = 13.9 Hz, $^5J_{F-F}$ = 6.9 Hz, 4-PhF), −162.46 (4F, dd, $^3J_{F-F}$ = 13.9 Hz, $^5J_{F-F}$ = 6.9 Hz, 2,6-PhF). UV–vis (c = 8.00 μM, DMSO, path length = 1 cm, 37 °C): λ /nm ($\varepsilon \times 10^{-4}/M^{-1}\,cm^{-1}$) = 414 (42.2), 507 (2.87), 534 (0.30), 581 (0.92). FL (c = 8.00 μM, DMSO, path length = 1 cm, λ_{ex} = 412.5 nm, 25 °C): λ/nm = 639, 704.

4.2.8. 5,15-Bis[4-(β-D-glucopyranosylthio)-2,3,5,6-tetrafluorophenyl)]-10,20-bis(2,3,4,5,6-pentafluorophenyl)porphyrin (*trans*-$\mathbf{2_{OH}}$)

A procedure similar to that described for $\mathbf{1_{OH}}$ as applied to ***trans*-$\mathbf{2_{Ac}}$** (23.2 mg, 13.9 μmol). The crude product was purified by column chromatography (Cosmosil®, acetonitrile/H_2O = 6:4) and washed with distilled water to give *trans*-$\mathbf{2_{OH}}$ (9.4 mg, yield 50.9%) as a dark red powder. Purity (HPLC): 98%. Anal. Calcd for $C_{56}H_{32}O_{10}N_4F_{18}S_2 + C_2H_3N + 3H_2O$: C, 48.99; H, 2.91; N, 4.92. Found: C, 49.20; H, 2.51; N, 5.08. ^{1}H NMR (600.17 MHz, CD_3OD, CHD_2OD = 3.30 ppm): δ (ppm) = 9.71, 9.18 (8H, br s, β-pyrroleH), 5.18 (2H, d, ^3J = 8.1 Hz, 1′-GlcH), 4.01 (2H, dd, ^3J = 11.8 Hz, ^2J = 1.6 Hz, 6′-GlcH), 3.78 (2H, dd, ^3J = 11.8 Hz, ^2J = 3.1 Hz, 6′-GlcH), 3.53–3.44 (8H, m, 2′,3′,4′,5′-GlcH). ^{13}C NMR (150.92 MHz, CD_3OD, CD_3OD = 49.0 ppm): δ (ppm) = 157.32–135.79 (α,β-pyrroleC, 2,6-PhC and 3,5-PhC), 121.74 (4-PhC), 116.71, 115.23 (1-PhC), 106.04, 104.81 (mesoC), 86.75 (1′-GlcC), 82.80 (5′′-GlcC), 79.77 (3′-GlcC), 75.99 (2′-GlcC), 71.75 (4′-GlcC), 63.11 (6′-GlcC). ^{19}F NMR (564.72 MHz, CD_3OD, CF_3CO_2H = −76.05 ppm): δ (ppm) = −132.68 (4F, dd, $^3J_{F-F}$ = 13.9 Hz, $^5J_{F-F}$ = 6.9 Hz, 3,5-PhFGlc), −137.72 (4F, dd, $^3J_{F-F}$ = 13.9 Hz, $^5J_{F-F}$ = 6.9 Hz, 3,5-PhF), −138.17 (4F, dd, $^3J_{F-F}$ = 13.9 Hz, $^5J_{F-F}$ = 6.9 Hz, 2,6-PhFGlc), −153.01 (2F, t, $^2J_{F-F}$ = 20.8 Hz, 4-PhF), −162.60 (4F, dd, $^3J_{F-F}$ = 13.9 Hz, $^5J_{F-F}$ = 6.9 Hz, 2,6-PhF). UV–vis (c = 8.00 μM, DMSO, path length = 1 cm, 37 °C): λ/nm ($\varepsilon \times 10^{-4}/M^{-1}\,cm^{-1}$) = 414 (32.8), 507 (2.15), 535 (0.21), 582 (0.70), 634 (0.07). FL (c = 8.00 μM, DMSO, path length = 1 cm, λ_{ex} = 413.5 nm, 25 °C): λ/nm = 639, 704.

4.2.9. 5,10,15-Tris[4-(β-D-glucopyranosylthio)-2,3,5,6-tetrafluorophenyl)]-20-bis(2,3,4,5,6-pentafluorophenyl)porphyrin ($\mathbf{3_{OH}}$)

A procedure similar to that described for $\mathbf{1_{OH}}$ as applied to $\mathbf{3_{Ac}}$ (47.9 mg, 23.9 μmol). The crude product was purified by column chromatography (Cosmosil®, acetonitrile/H_2O = 6:4) and washed with distilled water to give $\mathbf{3_{OH}}$ (20.0 mg, yield 52.4%) as a dark red powder. Purity (HPLC): >99%. Anal. Calcd for $C_{62}H_{43}O_{15}N_4F_{17}S_3 + 3H_2O$: C, 48.09; H, 3.28; N, 4.38. Found: C, 47.56; H, 3.04; N, 3.81. ^{1}H NMR (600.17 MHz, CD_3OD, CHD_2OD = 3.30 ppm): δ (ppm) = 9.17 (8H, br s, β-pyrroleH), 5.23 (3H, m, 1′-GlcH), 4.01 (3H, dd, ^3J = 12.0 Hz, ^2J = 1.4 Hz, 6′-GlcH), 3.78 (3H, dd, 3 J = 6.1 Hz, 2J = 3.1 Hz, 6′-GlcH), 3.56–3.43 (12H, m, 2′,3′,4′,5′-GlcH). ^{13}C NMR (150.92 MHz, CD_3OD, CD_3OD = 49.0 ppm): δ (ppm) = 149.48–146.84 (α,β-pyrroleC, 2,6-PhC and 3,5-PhC), 121.74 (4-PhC), 116.71, 115.23 (1-PhC), 106.04, 104.81 (mesoC), 86.75 (1′-GlcC), 82.80 (5′-GlcC), 79.77 (3′-GlcC), 75.99 (2′-GlcC), 71.75 (4′-GlcC), 63.11 (6′-GlcC). ^{19}F NMR (564.72 MHz, CD_3OD, CF_3CO_2H = −76.05 ppm): δ (ppm) = −132.68 (6F, dd, $^3J_{F-F}$ = 13.9 Hz, $^5J_{F-F}$ = 6.9 Hz, 3,5-PhFGlc), −137.70 (2F, d, $^3J_{F-F}$ = 20.8 Hz, 3,5-PhF), −138.11 (6F, dd, $^3J_{F-F}$ = 13.9 Hz, $^5J_{F-F}$ = 6.9 Hz, 2,6-PhFGlc), −153.04 (1F, dd, $^3J_{F-F}$ = 13.9 Hz, $^5J_{F-F}$ = 6.9 Hz, 4-PhF), −162.60 (2F, dd, $^3J_{F-F}$ = 13.9 Hz, $^5J_{F-F}$ = 6.9 Hz, 2,6-PhF). UV–vis (c = 8.00 μM, DMSO, path length = 1 cm, 37 °C): λ /nm ($\varepsilon \times 10^{-4}/M^{-1}\,cm^{-1}$) = 415 (27.8), 507 (1.78), 537 (0.17), 581 (0.57), 633 (0.09). FL (c = 8.00 μM, DMSO, path length = 1 cm, λ_{ex} = 413.5 nm, 25 °C): λ/nm = 640, 705.

4.3. $^1O_2$ Generation efficiency

S-Glucosylated porphyrins (c = 0.86 μM) and DPBF (c = 111 μM) were dissolved in DMSO and the solution was added a square quartz cell (1 cm). Prior to photoirradiation, oxygen gas was introduced through the solution for 1 min. The solution was then exposed to light from a 100 W halogen lamp (KBEX-102A, USHIO Inc., Tokyo, Japan) through a Y-50 cut-off filter (λ >500 nm, Toshiba Co., Tokyo, Japan) at 37 °C. The concentration of DPBF was monitored by measuring the absorption at 418 nm. The rate constant

k (s^{-1}) was estimated from the first-order plot of the DPBF concentration against the photoirradiation time.

4.4. Reactive oxygen radical species generation efficiency

S-Glucosylated porphyrins $\mathbf{1}_{OH}$, *cis*-$\mathbf{2}_{OH}$, *trans*-$\mathbf{2}_{OH}$, $\mathbf{3}_{OH}$ and $\mathbf{4}_{OH}$ (c = 1.00 μM) and DCFDA (c = 2 μM) were dissolved in PBS solution containing 3 vol % DMSO and the solution was added a sample tube. The solution was then exposed to light from a 100 W halogen lamp (KBEX-102A, USHIO Inc., Tokyo, Japan) through a Y-50 cut-off filter (λ >500 nm, Toshiba Co., Tokyo, Japan) at 37 °C. The initial rate of DCFDA fluorescence intensity increments was monitored by measuring the excitation and emission wavelengths at 430 and 635 nm. The rate constant was estimated from the first-order plot of DCFDA fluorescence intensity increments against photoirradiation time.

4.5. Hydrophobicity parameters by RP-TLC method

Hydrophobicity parameter (logarithm of partition coefficient between *n*-octanol and water; Log *P*) is well-correlated with the capacity factor k' in reverse-phase (i.e., partition) chromatography as follows,

$$\mathrm{Log}\,P = a\mathrm{Log}\,k' + b \quad (1)$$

where a and b are constants for a given chromatographic system. The capacity factor k' was determined by the R_f value in reverse-phase thin layer chromatography (RP-TLC) using octadecylsilyl-bound silica gel (R-18F_{254s}, Merck Japan Ltd, Tokyo, Japan) and a mixture of CH_3OH and H_2O (9/1, v/v) as an eluent as follows,

$$k' = 1/R_f \quad (2)$$

Benzaldehyde (Log *P* = 1.48), benzophenone (3.20), *m*-hydroxybenzaldehyde (1.25), *p*-fluorobenzaldehyde (1.39) and *m*-fluorobenzaldehyde (1.89) were used as standards to calibrate our RP-TLC system.

4.6. In vitro cellular uptake measurement

HeLa cells (ATCC CCL-2) were obtained from Dainippon-Sumitomo Pharmaceutical (Osaka, Japan). They were grown in Dulbecco's modified Eagle's medium (DMEM) containing 10% fetal calf serum (FCS) (Hyclone Laboratories, Inc., Logan, UT). The cellular uptake of deprotected S-glucosylated photosensitizers by HeLa cells was examined as follows: HeLa cells (1×10^6 cells/well) in 1.5 mL of DMEM containing 10% FCS were plated in a 6-well plate (Nalge Nunc International, Naperville, IL) and incubated for 24 h (37 °C, 5% CO_2). One point five milliliters of 80 nM photosensitizer in DMEM containing 10% FCS and 2% DMSO was added to each well, and the plate was incubated for 24 h. The photosensitizer concentration was 160 nM in DMEM containing 10% FCS (final DMSO content was 1% in all cases). The cells were then washed twice with Dulbecco's phosphate-buffered saline (PBS). The cells were lysed in 150 μL of DMSO. The absorption at Soret band was measured with UV–vis spectrophotometer. The concentration of photosensitizer was calculated on the basis of calibration plots obtained for each photosensitizer in DMSO. The cellular uptake amounts are given as the means of results from three replicate experiments.

4.7. In vitro photocytotoxicity test

The photocytotoxicity of the S-glucosylated photosensitizers in HeLa cells was examined as follows: HeLa cells (5×10^3 cells) in 100 μL of DMEM containing 10% FCS were plated in a 96-well plate (Nalge Nunc International) and incubated for 24 h (37 °C, 5% CO_2). One hundred microliters of a photosensitizer in DMEM containing 10% FCS and 2% DMSO was added to each well. The plate was then incubated from 24 h in the presence of the photosensitizers. The photosensitizer concentration was varied from 500 to 1 nM in DMEM containing 10% FCS (final DMSO content was 1% in all cases). The cells were washed twice with PBS, and then 100 μL of DMEM containing 10% FCS was added. The cells were exposed to light from a 100 W halogen lamp equipped with a water jacket and a Y-50 cut-off filter. The light intensity was measured by using a UV–vis power meter (ORION/TH, Ophir Optronics Ltd, Jerusalem, Israel). The irradiation time was adjusted to obtain the desired light dose of 16 J cm^{-2}. The mitochondrial activity of NADH dehydrogenase of the cells in each well was measured at 24 h after photoirradiation using WST-8® reagent (10 μL) from Cell Counting Kit-8 (Dojindo, Tokyo, Japan) according to the manufacturer's instructions. The absorbance at 450 nm was measured using a plate reader. The percentage cell survival was calculated by normalization with respect to the value for no drug treatment.

4.8. Confocal laser-scanning microscopy

HeLa cells (1×10^4 cells) in 500 μL of DMEM containing 10% FCS were plated in two 24-well plates, and incubated for 24 h (37 °C, 5% CO_2). Five hundred microliters of 1.0 μM photosensitizer in DMEM containing 10% FCS and 2% DMSO was added to each well, and then incubation was continued for 24 h in the presence of the photosensitizers. The final concentration of photosensitizers was 500 nM (1% DMSO). The cells in one 24-well plate were washed twice with 500 μL of PBS, and 500 μL of Hank's balanced salt solution (HBSS) was added to each well. Fluorescence images of photosensitizers in cells were taken with the CLSM using an excitation wavelength of 488 nm. For the other plate, on the other hand, 500 μL of DMEM containing 10% FCS was added to each well instead of HBSS. Then each well was photoirradiated under the same conditions as described in the previous section. Three hours after photoirradiation, the cells were stained with DAPI 0.3 μM PBS for 5 min at room temperature, and then washed twice with 500 μL of PBS, and finally 500 μL of HBSS was added. Fluorescence images of DAPI-stained cells were taken using an excitation wavelength of 364 nm.

4.9. Statistical analysis

All statistical evaluations were performed using Student's *t*-test. All values for cellular uptake and cytotoxicity are expressed as mean ± standard deviation.

Acknowledgements

This work was supported by the NAIST Presidential Special Fund (S.H.), Grants-in-Aid for Scientific Research and Priority Areas from the Ministry of Education, Culture, Sport, Science and Technology (MEXT) of the Japanese Government, Sasagawa Scientific Research Grants from The Japan Science Society (M.O.), a Nara Women's University Intramural Grant for Project Research (M.O.) and grants from The Kao Foundation for Arts and Sciences (M.O.). The authors thank Professor Shigenobu Yano of Kyoto university for helpful discussion and kindly support.

References and notes

1. Kessel, D. *Photodiagn. Photodyn. Ther.* **2004**, *1*, 3.
2. Castano, A. P.; Demidova, T. N.; Hamblin, M. R., PhD *Photodiagn. Photodyn. Ther.* **2004**, *1*, 279.
3. Castano, A. P.; Demidova, T. N.; Hamblin, M. R., PhD *Photodiagn. Photodyn. Ther.* **2005**, *2*, 1.

4. Castano, A. P.; Demidova, T. N.; Hamblin, M. R., PhD *Photodiagn. Photodyn. Ther.* **2005**, *2*, 91.
5. Detty, M. R.; Gibson, S. L.; Wagner, S. J. *J. Med. Chem.* **2004**, *47*, 3897.
6. Macdonald, I. J.; Dougherty, T. J. *J. Porphyrins Phthalocyanines* **2001**, *5*, 105.
7. Kessel, D.; Thompson, P.; Saatio, K.; Nantwi, K. D. *Photochem. Photobiol.* **1987**, *45*, 787.
8. Spikes, J. D.; Bommer, J. C. *Photochem. Photobiol.* **1987**, *45*, 798.
9. Berg, K.; Western, A.; Bommer, J. C.; Moan, J. *Photochem. Photobiol.* **1990**, *52*, 487.
10. Berg, K.; Bommer, J. C.; Winkelman, J. W.; Moan, J. *Photochem. Photobiol.* **1990**, *52*, 775.
11. Momenteau, M.; Maillard, P.; de Bélinay, M.-A.; Carrez, D.; Croisy, A. *J. Biomed. Opt.* **1999**, *4*, 298.
12. Laville, I.; Figueiredo, T.; Loock, B.; Pigaglio, P.; Maillard, P.; Grierson, D. S.; Carrez, D.; Croisy, A.; Blais, J. *Bioorg. Med. Chem.* **2003**, *11*, 1643.
13. Kashiwagi, Y.; Imahori, H.; Araki, Y.; Ito, O.; Yamada, K.; Sakata, Y.; Fukuzumi, S. *J. Phys. Chem. A* **2003**, *107*, 5515.
14. Defaye, J.; Driguez, H.; Ohleyer, E.; Orgeret, C.; Viet, C. *Carbohydr. Res.* **1984**, *130*, 317.
15. Rosenberger, V.; Margalit, R. *Photochem. Photobiol.* **1993**, *58*, 627.
16. Zheng, G.; Potter, W. R.; Sumlin, A.; Dougherty, T. J.; Pandey, R. K. *Bioorg. Med. Chem. Lett.* **2000**, *15*, 123.
17. Rungta, A.; Zheng, G.; Missert, J. R.; Potter, W. R.; Dougherty, T. J.; Pandey, R. K. *Bioorg. Med. Chem. Lett.* **2000**, *10*, 1463.
18. Zheng, G.; Potter, W. R.; Camacho, S. H.; Missert, J. R.; Wang, G.; Bellnier, D. A.; Henderson, B. W.; Rodgers, M. A. J.; Dougherty, T. J.; Pandey, R. K. *J. Med. Chem.* **2001**, *44*, 1540.
19. McCall, J. M. *J. Med. Chem.* **1975**, *18*, 549.
20. Kaliszan, R. *J. Chromatogr.* **1981**, *220*, 71.
21. Miyake, K.; Terada, H. *J. Chromatogr.* **1982**, *240*, 9.
22. OECD GUIDELINE FOR TESTING OF CHEMICALS, 1989, 117.
23. Calculated using Advanced Chemistry Development (ACD/Labs) Software V8.14 for Solaris (©1994–2009 acd/Labs).
24. Hirohara, S.; Obata, M.; Alitomo, H.; Sharyo, K.; Ando, T.; Yano, S.; Tanihara, M. *Bioconjugate Chem.* **2009**, *20*, 944.